Metrol. Meas. Syst., Vol. 24 (2017), No. 2, pp. 425–436.

METROLOGY AND MEASUREMENT SYSTEMS
Index 330930, ISSN 0860-8229
www.metrology.pg.gda.pl

EFFECT OF ADC RESOLUTION ON LOW-FREQUENCY ELECTRICAL TIME-DOMAIN IMPEDANCE SPECTROSCOPY

Reyhaneh L. Namin, Shahin J. Ashtiani

University of Tehran, College of Engineering, P.O. Box 14395/515 Tehran, Iran
(latifi.re@gmail.com, ✉ sashtiani@ut.ac.ir, +98 21 8208 4952*)*

Abstract

In this paper, the effect of the resolution of an *analogue-to-digital converter* (ADC) on the accuracy of time-domain low-frequency electrical impedance spectroscopy is examined. For the first time, we demonstrated that different wideband stimuli signals used for impedance spectroscopy have different sensitivities to the resolution of ADC used in impedance spectroscopy systems. We also proposed Ramp and Half-Gaussian signals as new wideband stimulating signals for EIS. The effect of ADC resolution was studied for Sinc, Gaussian, Half-Gaussian, and Ramp excitation signals using both simulation and experiments. We found that Ramp and Half-Gaussian signals have the best performance, especially at low frequencies. Based on the results, a wideband electrical impedance spectroscopy circuit was implemented with a high accuracy at frequencies bellow 10 Hz.

Keywords: electrical impedance spectroscopy, analogue-to-digital converter, Ramp signal, Fast Furrier transform, Nyquist plot.

1. Introduction

Electrical impedance spectroscopy (EIS) is a non-destructive, inexpensive and simple measurement method for testing properties of electrochemical or biological systems [1].This technique is widely used in several industrial and biological applications such as corrosion monitoring [2], study of the solar cells [3] fuel cells [4] and batteries [5], distinction between normal and cancerous cells [6], and measurement of flowing blood to predict white thrombus formation [7].

The spectrum of impedance is a Nyquist plot, consisting of points that describe the magnitude and phase of the impedance for a specific frequency. The spectrum shape characterizes the order, structure, and the equivalent electrical model of a sample under test.

In EIS, the precision, frequency range, and test duration are very important. Since there is a possibility of change in the structure of the sample under test due to applying an excitation signal for a long time, the duration of EIS has a high significance, particularly in studying biomaterials and medical applications.

The frequency range in which EIS is performed is determined by the sample. For instance, while in medicine the desired frequency range can be in the range of hundreds to a few thousand Hertz, it can be as low as a few mili-Hertz in battery and fuel cell applications [8, 9].

There are two general techniques used in EIS: the frequency domain and the time domain. In the frequency domain spectroscopy, a frequency is the independent variable and the excitation signal is sinusoidal. To produce the impedance spectrum, the sinusoidal signal frequency is swept in the desired range [1].

While applying a sinusoidal excitation signal to the tested sample is one of the most comprehensive and simplest methods for extraction of the impedance spectrum, it takes a long

Article history: received on Feb. 17, 2016; accepted on Oct. 22, 2016; available online on Jun. 30, 2017; DOI: 10.1515/mms-2017-0019.

test time, especially at frequencies under 1 Hz [10]. Another issue of the method is its discrete frequency components: for each desired test frequency, at least one period of sinusoidal signal in that frequency should be applied to the sample. Therefore, the number of frequency steps in the impedance spectrum is associated with the number of sinusoidal signals that are applied to the sample under test. This results in lengthened test times, especially in low frequency ranges.

In the time domain spectroscopy, time is the independent variable. To extract the impedance as a function of frequency, a time-to-frequency transformation is needed. The transformation methods are generally based on Fourier [4], Laplace [11] or Wavelet [12] transforms. The excitation in the time domain spectroscopy is a wideband signal such as a multi-sinusoidal, chirp, Sinc signal [10], a pulse or white noise [12]. An advantage of using a wideband signal is that by applying a single excitation, the impedance spectrum of the entire desired frequency range can be obtained at once. This results in faster obtaining a more accurate spectrum, especially in low frequency ranges.

Since time-to-frequency transformations have to be done in the digital domain, an *analogue-to-digital converter* (ADC) should be used. The resolution and sampling frequency of ADC has a significant effect on a precision of the impedance spectrum. If the ADC has an infinite resolution and sampling frequency, the impedance spectrum has no error. However, in practice, using an ADC with a limited resolution and sampling frequency causes an error in the resulted impedance spectrum.

The ADC error associated with the limited resolution is generally modelled by the quantization noise. The general quantization noise theory predicts that the ADC error due to a limited resolution is almost independent of the input signal and it just depends on the resolution [13]. However, our findings based on simulations and experimental results for the first time show that the shape of the excitation signals used in time domain EIS, has a significant effect on the error of the measured impedance, when the ADC resolution is limited.

In this paper, we examine the effect of ADC resolution on the error of the measured impedance for several excitation signals, including Sinc, Gaussian, and half-Gaussian ones. In addition, we propose Ramp as a simple and accurate excitation signal for the time domain EIS with a low sensitivity to ADC resolution. The purpose of this paper is – using a specific hardware – to find an excitation signal which can result in an impedance spectrum with less errors.

In the next section, some excitation signals including the Ramp one, are introduced. In the third section, the proposed method of implementing a wide-band impedance spectroscopy measurement system is presented. Finally, the results of the measurements are reported, compared and analysed.

2. Excitation signals

To obtain an impedance spectrum, a small alternate current or voltage as the excitation signal is applied to the sample and the response signal is monitored and measured. The ratio of the *Fast Furrier Transform* (FFT) of the response signal and the FFT of the excitation signal, as a transfer function, indicates the sample impedance.

Selection of an appropriate excitation signal – especially at low frequencies – is an important issue in EIS. A multi-sinusoidal excitation signal has been used in some previous research works [5]. This signal consists of 10 to 15 frequencies and the duration of applying the signal is equal to the period of its lowest frequency. Using a multi-sinusoidal signal results in a shorter measurement time, in comparison with sinusoidal signals. A disadvantage of the multi-sinusoidal signal is its discrete frequency components and elevated amplitudes.

In some previous works a pulse signal is used as the excitation signal. It has a continuous frequency spectrum. However, its high-frequency components drop off rapidly, resulting

in a lower accuracy at higher frequencies [14]. Moreover, for some specific frequencies, the amplitudes of its components are equal to zero.

A chirp excitation signal is also used in impedance spectroscopy systems. An advantage of using this signal is its independent scalability in frequency and time. While it is an appropriate signal for EIS at higher frequencies, it is not very accurate at low frequencies [12].

In this work, we used four excitation signals including Sinc, Gaussian, half-Gaussian and Ramp ones for comparison. Fig. 1 shows the signals in the time and frequency domains. All of these four signals have the same energy.

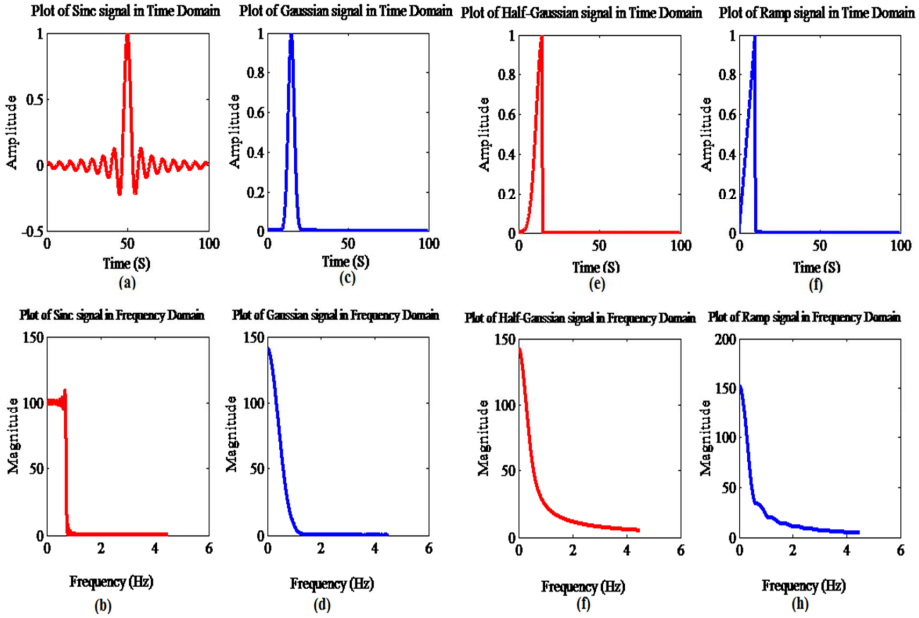

Fig. 1. Sinc, Gaussian, half-Gaussian and Ramp signals in the time and frequency domains.

Equations (1) to (4) define Sinc, Gaussian, Half-Gaussian and Ramp signals, respectively:

$$Sinc(t) = \frac{\sin(2\pi(t-50))}{2\pi(t-50)}, \tag{1}$$

$$Gaussian(t) = e^{\frac{-(t-15)^2}{2\sigma^2}}, \quad \sigma = 0.98, \tag{2}$$

$$Half-Gaussian(t) = \begin{cases} e^{\frac{-(t-15)^2}{2\sigma^2}} & t<15 \\ 0 & t>15 \end{cases}, \quad \sigma = 2, \tag{3}$$

$$Ramp(t) = \begin{cases} \frac{1}{15} * t & t < 15 \\ 0 & t > 15 \end{cases}. \tag{4}$$

Because of the presence of ADC and DAC the excitation signal is not ideal and the resolution and sampling frequency of ADC and DAC cause an error in the impedance spectrum. To extract the impedance spectrum for frequencies below 1 Hz, the excitation signal should have a high amplitude in the time domain. Also, the excitation signal in the frequency domain should have a sufficient magnitude in a wide range of frequencies.

Figures 1a and 1b show a Sinc signal in the time and frequency domains, respectively. As can be seen, an amplitude of the Sinc signal in the time domain drops

rapidly. As a result, an ADC with a high resolution and sampling frequency is required. In the frequency domain, the Sinc signal has an almost flat frequency spectrum but with a small value compared with other tree signals. In Figs. 1c and 1d a Gaussian signal in the time and frequency domains is shown. An amplitude of the Gaussian signal in the time domain is higher and is changing slower than that of the Sinc signal. A magnitude of the Gaussian signal in the frequency domain is higher at lower frequencies and an increase of the frequency causes a decrease of its magnitude, eventually dropping its value to zero. Figs. 1e and 1f show a half-Gaussian signal in the time and frequency domains. This signal is almost similar to the Gaussian one, but in the frequency domain its magnitude drops to zero in higher frequencies.

In Figs. 1g and 1h a Ramp signal in the time and frequency domains is shown. This signal has a higher amplitude in the time domain, and it also has a very high frequency-domain magnitude at very low frequencies and its magnitude decreases by increasing the frequency. But, like the half-Gaussian signal, its magnitude drops to zero in frequencies higher than those for the Gaussian signal.

3. Effect of ADC quantization on impedance spectrum

As mentioned earlier, in the time domain EIS, the impedance signal should be converted to a digital one by an ADC. In this section, we briefly study the effect of the ADC resolution and an excitation signal on the accuracy of the impedance spectrum. To do this, an excitation signal with 3000 samples in 100 s, with a rate of 30 S/s, is applied to the first-order impedance, and then the response signal is quantized by a 14-bit ADC model in MATLAB. The difference between the quantized signal at the ADC output and the input signal is calculated and then normalized to the amplitude of the *least significant bit* (LSB) of the ADC. Fig. 2 shows the simulated quantization errors for Sinc, Gaussian, half-Gaussian and Ramp signals in the time domain. As can be seen, the quantization error of the Sinc signal has a larger value and exists in the entire duration of sampling. One explanation for the higher error of the Sinc signal is the abrupt reduction in its time-domain amplitude. As a result, for a considerable part of the test duration, the signal amplitude goes well below the resolution of the ADC. While Gaussian, half-Gaussian and Ramp signals have non-perfect frequency spectra compared with the Sinc signal, they have a smoother shape in the time-domain and for most of the test duration their amplitudes are large enough to be detected by the ADC.

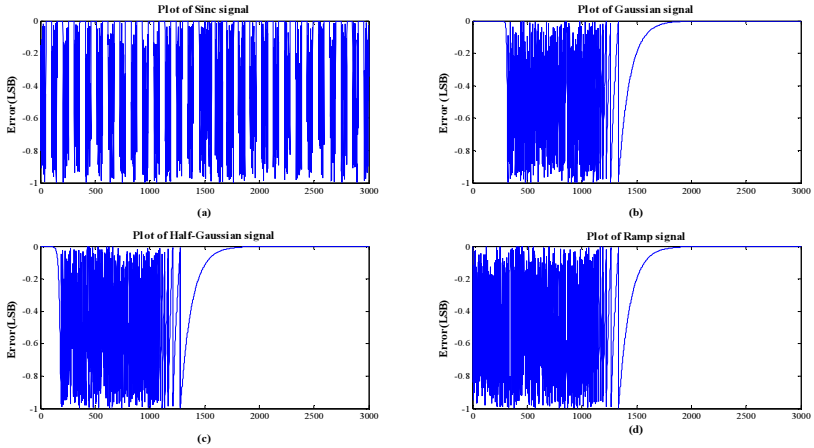

Fig. 2. The time-domain quantization error of Sinc, Gaussian, half-Gaussian and Ramp signals. The errors are normalized to the amplitude of the *least significant bit* (LSB) of the ADC.

For comparison, the *root mean square* (RMS) and mean quantization errors of the four signals in LSB, are calculated and listed in Table 1.

Table 1. The RMS and mean quantization errors of Sinc, Gaussian, half-Gaussian and Ramp signals.

Signal	Mean error (normalized to LSB)	RMS error (Normalized to LSB)
Sinc	–0.4608	0.3228
Gaussian	–0.2428	0.1678
half-Gaussian	–0.2147	0.1353
Ramp	–0.2586	0.1664

As can be seen, the smallest quantization error is that of the half-Gaussian signal. The Ramp and Gaussian signals also have lower errors compared with the Sinc one.

To examine the effect of ADC on the impedance spectrum, Nyquist plots of the first-order impedance using the previous excitation signals are obtained by simulation using MATLAB. In the simulations, the ADC has a 14-bit resolution, its sampling frequency is 30 S/s, and a duration of applying the excitation signal is 100 s.

To obtain the electrical impedance spectrum in MATLAB, the excitation signal is quantized and the FFT of the excitation signal is calculated, then this signal applied to the sample is again quantized and the FFT of the response is calculated. Eventually, by using some math operations, the impedance spectrum is extracted.

Figure 3 shows the sample circuit which has been used in the simulations. Table 2 contains the values of components used in the simulations.

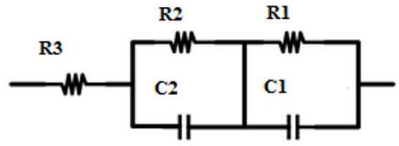

Fig. 3. The sample impedance circuit used for the measurements and simulations.

Table 2. The component values used in the simulations.

R1	R2	R3	C1	C2
0.5 KΩ	0.5 KΩ	0.5 KΩ	6.8 mF	10 uF

Figure 4 shows the simulation results. The ideal Nyquist plot is shown by the blue dots, whereas the red dots represent the impedance spectrum obtained from the simulation.

According to the Nyquist plots resulted from Sinc, Gaussian, half-Gaussian and Ramp excitation signals, we perceive that the impedance spectrum errors for the Ramp and half-Gaussian excitation signals are lower than the error which have been obtained by other excitation signals.

The effect of reduction of the ADC resolution on the impedance error is studied. Figs. 5 and 6 show average magnitude and phase errors of the impedance spectrum as a function of the ADC resolution. As can be seen, for the Sinc signal, both phase and magnitude errors of the impedance considerably increase with decreasing the ADC resolution. The lowest sensitivity to the ADC resolution can be achieved by using Ramp or half-Gaussian signals.

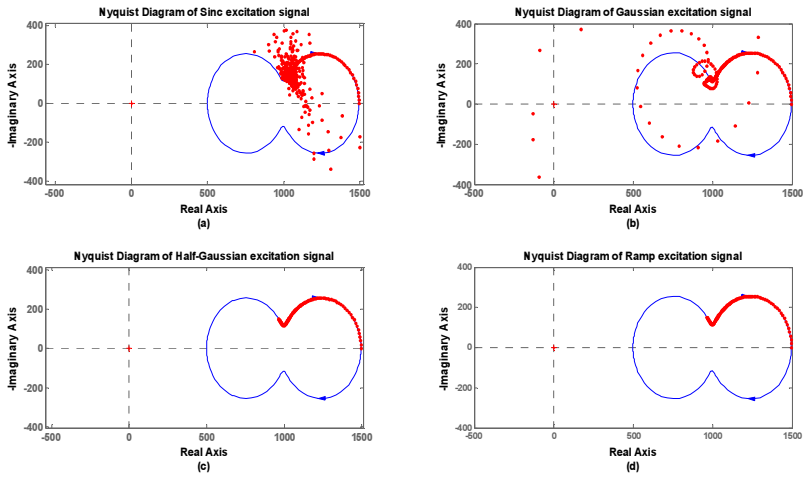

Fig. 4. The Nyquist plots of the first-order sample obtained with Sinc (a); Gaussian (b); half-Gaussian (c); Ramp excitation signals (d).

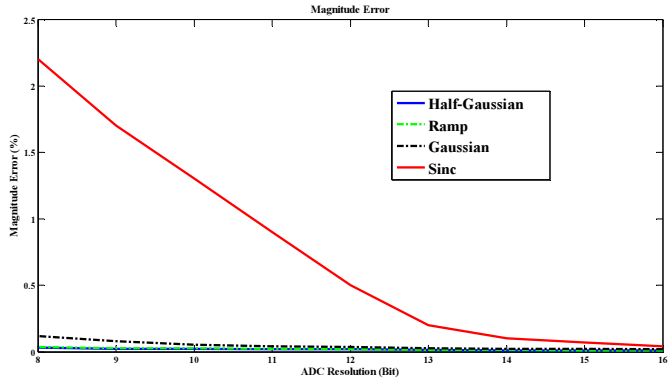

Fig. 5. The average magnitude error of simulated impedance spectrum as a function of the ADC resolution for different excitation signals.

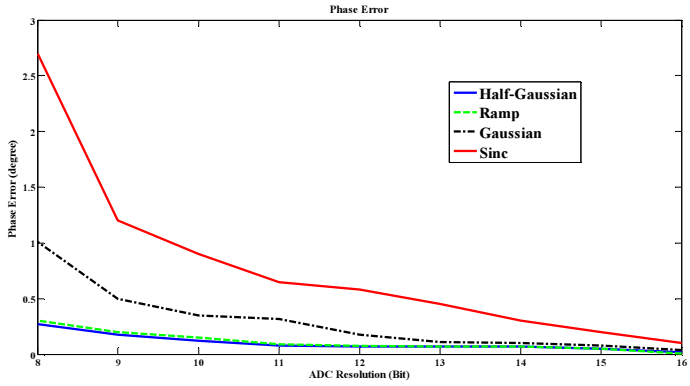

Fig. 6. The average phase error of simulated impedance spectrum as a function of the ADC resolution for different excitation signals.

4. Measurement and Test Setup

4.1. Design of Test Circuit

To test the effect of the ADC quantization error on the impedance spectrum for the four excitation signals, a test circuit has been designed. Impedance analyser designs use either custom circuits [15] or application-specific *integrated circuits* (ICs), such as AD5833 [16]. In our case, since we need to study the effect of ADC resolution, we designed a simple specific circuit with monolithic ADC and DAC ICs. Fig. 7 shows a block diagram of the test circuit. The circuit has analogue and digital sections. The analogue circuitry regulates the voltage applied to the sample and monitors the output current from the sample under test. It contains op-amps U1-U5 and an instrumentation amplifier U6. The digital section executes signal processing and calculates the Fast Fourier transform.

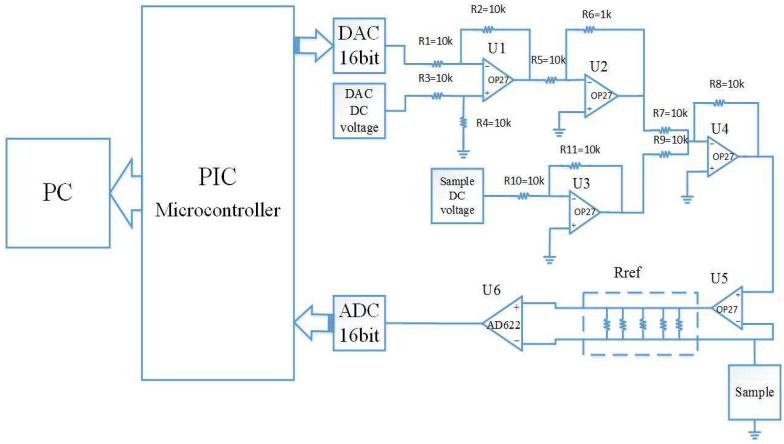

Fig. 7. A block diagram of the electrical impedance spectroscopy system.

An excitation signal is generated by a microcontroller in the digital domain and is converted to an analogue form by a *digital-to-analogue converter* (DAC). The amplitude signal is set by U2. Since a wide range of samples are non-linear, and because the Fast Fourier transform can be used only for linear systems, the amplitude of excitation signal should be small. In some cases it is necessary to bias the sample with a specific DC voltage. U3 provides the DC voltage. U4 acts as a summing circuit and adds the DC and AC voltages. The excitation voltage is applied to the sample by U5. The sample is placed between the inverting input of U5 and the ground. When the excitation voltage is applied to the sample, a current passes through the sample and then flows into the reference resistors. According to the impedance range of the sample, one of the reference resistors is selected and the current passes through it. The voltage across the reference resistor has a linear relationship with the current passing through the sample. This voltage is amplified by the instrument amplifier U6. The output of the instrument amplifier is connected to the analogue-to-digital converter, and afterwards the digital data are sent to the microcontroller for processing. The ADC resolution is 16 bits, but the effective number of bits is 14 bits.

Since the DAC output voltage is only positive, the DAC DC voltage source is used to adjust the DC level of the excitation signal. In addition, in some EIS applications – such as measurement of batteries and fuel or electrochemical cells – there is a need for a constant DC bias. In this case, the sample DC voltage along with the DAC DC voltage sources provide the required DC bias for the sample.

In the microcontroller, FFT of the response is calculated and used in the calculated FFT of the excitation signal. In this case, the input signal is a voltage one and the output signal is a current one. Therefore, the transfer function represents the admittance of the sample under test. It is necessary to reverse the transfer function to obtain the impedance of the sample.

The DAC used in this system is AD5663 with a resolution of 16 bits. Op-amps U1-U4 are OP27 with a low offset voltage. AD620 is selected as the instrument amplifier due to its low offset and noise level. The noise associated with the analogue electronic components, including the U1 to U6 and resistors at the ADC input, is simulated with SPICE. It is close to 850 nV rms which is much lower than the LSB of ADC. The selected ADC type is AD7988-5 that has a sampling frequency of up to 500 kHz. The PIC33Fj128GP804 microcontroller type is used in this prototype for digital calculations. Fig. 8 illustrates the circuit board of complete test circuit for impedance spectrum measurement.

Fig. 8. The circuit board of the electrical impedance spectroscopy system.

To transfer data from the microcontroller to PC and to plot the impedance spectrum, a USB interface is used. By deploying the serial interface, the real and imaginary parts of impedance are separately sent to the computer and – with help of MATLAB – Nyquist plots of the measured impedance of samples are drawn.

4.2. Measurement results

To calculate the magnitude and phase errors of impedance spectrum, Sinc, Gaussian, half Gaussian and Ramp excitation signals are applied to the sample circuit shown in Fig. 3. The values of components used in this measurement are the same as those in simulation, which is shown in Table 2. The impedance spectrum for various resolutions of the ADC is calculated. Figs. 9 and 10 show the RMS error in the measured impedance spectrum phase and magnitude versus the ADC resolution.

Figure 11 shows the impedance spectrum extracted by all the four excitation signals presented in Fig. 1.

As indicated in Fig. 11, the RMS error of the impedance spectra which are obtained from the Ramp and half-Gaussian excitation signals are much smaller than the error obtained from the Sinc excitation signal. As a result of reduction of the ADC resolution, the impedance spectrum error from the Sinc excitation signal has a faster increase rate. It should be noted that the errors are obtained for the frequency range of 5 mHz to 10Hz. In all measurements, an ADC sampling frequency is set to 30 S/s. Also, the DAC generates data at a rate of 30 S/s.

Finally, in order to obtain the impedance spectrum in a wide range of frequencies and also reducing the measurement points, three separate excitation signals were applied to the sample. The first excitation signal was applied to the sample for 100 seconds and its impedance spectrum in the frequency range of 5 mHz to 10 Hz is illustrated by the red circles in Fig. 12. The second excitation signal was applied to the sample for 1 s, which presents the frequency range of 10 Hz to 100 Hz and is shown with the black squares. Finally, the last excitation signal is also applied for 1 ms and its impedance spectrum frequency is up to 600 Hz and is displayed by the blue triangles. Fig. 12 shows the Nyquist plot obtained from these three excitation signals.

The reason of applying several excitation signals is that by using only one excitation signal for a wide range of frequencies, the FFT of signal is calculated with a fixed N; therefore for higher frequencies the number of FFT points increases and thus the process takes a long time.

The sample circuit used for this measurement is shown in Fig. 2, and the values of components are shown in Table 3.

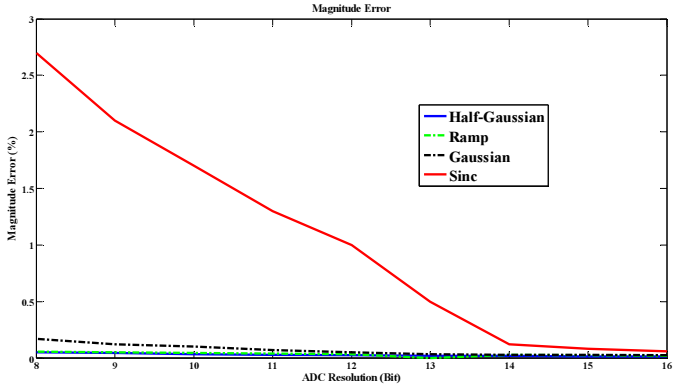

Fig. 9. The magnitude error of the measured impedance spectrum.

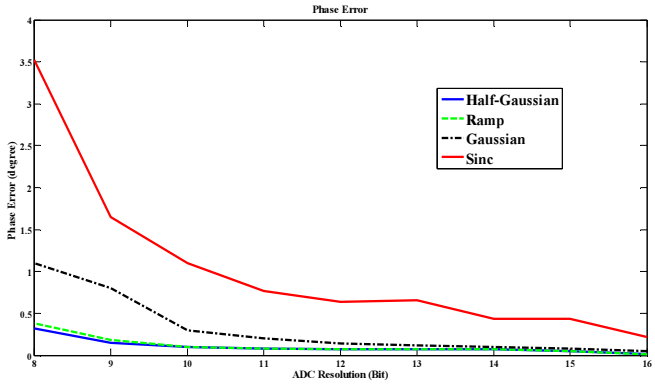

Fig. 10. The phase error of the measured impedance spectrum.

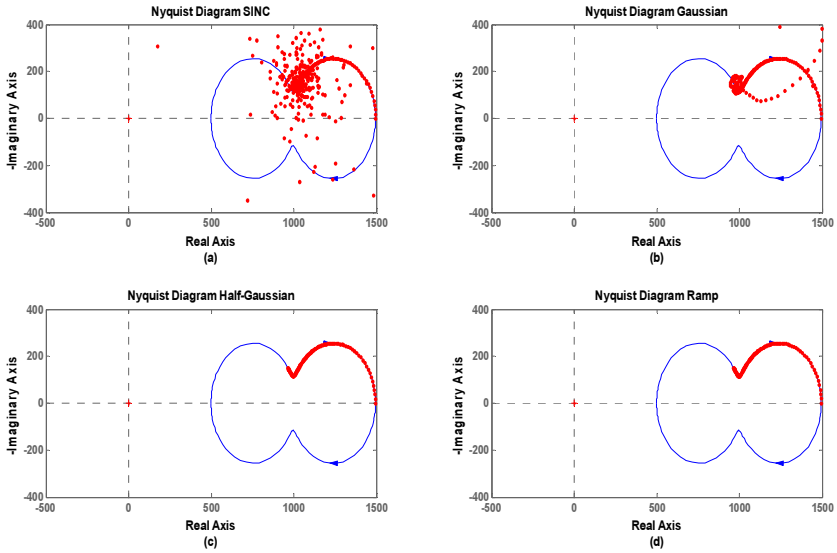

Fig. 11. The Nyquist plots extracted from measurement by using Sinc, Gaussian, half-Gaussian and Ramp excitation signals.

Table 3. The values of components used for measurement of the impedance spectrum by using several excitation signals.

R1	R2	R3	C1	C2
1 KΩ	1 KΩ	1 KΩ	6.8 mF	10 uF

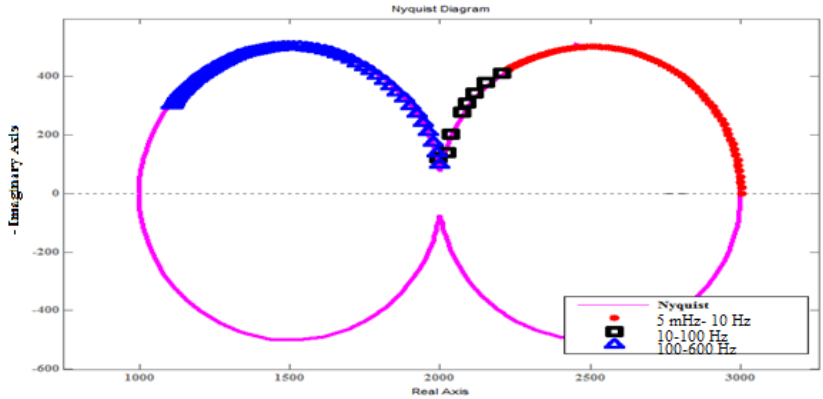

Fig. 12. The Nyquist plot of the second-order sample obtained with 3 separate excitation signals.

5. Conclusion

In this paper, the effect of ADC resolution and the excitation signal shape in the time domain impedance spectroscopy are for the first time studied simultaneously. We found that the excitation signal shape and the ADC resolution have a significant impact on the accuracy of the measured

impedance spectrum. Several excitation signals are used in the time domain impedance spectroscopy, such as Sinc and Gaussian ones. In this paper Ramp and half-Gaussian signals are also studied for the first time. These two new excitation signals are compared with the Sinc and Gaussian ones to figure out which of them generate a more accurate impedance spectrum when the ADC resolution is limited. By applying all the four excitation signals for 100 s, the impedance spectra of each of them for a frequency range from 5 mHz to 5 Hz are extracted. Based on the simulation and measurement results, the Ramp and half-Gaussian excitation signals result in lower RMS errors than those obtained from the Sinc and Gaussian signals. Also, with reduction of ADC resolution, an increase of the impedance spectrum error is higher than resulted from other signals.

Reference

[1] Lvovich, V.F. (2012). *Impedance spectroscopy: applications to electrochemical and dielectric phenomena.* John Wiley & Sons.

[2] Hoja, J., *et al.* (2011). Method using square pulse excitation for high-impedance spectroscopy of anticorrosion coatings. *IEEE Trans. Instrum. Meas.*, 60(3), 957–964.

[3] Lohrasbi, M., *et al.* (2013). Degradation study of dye-sensitized solar cells by electrochemical impedance and FTIR spectroscopy. *Proc. of IEEE Energytech 2013*, Cleveland OH, US, 1–4.

[4] Debenjak, A., *et al.* (2012). An assessment of water conditions in a PEM fuel cell stack using electrochemical impedance spectroscopy. *IEEE PHM 2012*, Beijing, China, 23–25.

[5] Lindahl, P.A., *et al.* (2012). A time-domain least squares approach to electrochemical impedance spectroscopy. *IEEE Trans. Instrum. Meas.*, 61(12), 3303–3311.

[6] Kang, G., *et al.* (2012). Differentiation between normal and cancerous cells at the single cell level using 3-D electrode electrical impedance spectroscopy. *IEEE Sensors J.*, 12(5), 1084–1089.

[7] Affanni, A., *et al.* (2012). Electrical impedance spectroscopy on flowing blood to predict white thrombus formation in artificial microchannels. *IEEE I2MTC 2012*, Graz, Autria, 1477–1480.

[8] Sanchez, B., Vandersteen, G., Rosell-Ferrer, J., Cinca, J., Bragos, R. (2011). In-cycle myocardium tissue electrical impedance monitoring using broadband impedance spectroscopy. *Engineering in Medicine and Biology Society, EMBC, 2011,* Boston, US, 2518–2521.

[9] Rojo, L., Mandayo, G.G., Castafio, E. (2013). Thin film YSZ solid state electrolyte characterization performed by electrochemical impedance spectroscopy. *Spanish Conference on Electron Devices (CDE)*, Valladolid, Spain, 233–236.

[10] Kowalewski, M., Lentka, G. (2013). Fast high-impedance spectroscopy method using sinc signal excitation. *Metrol. Meas. Syst.*, 20(4), 645–654.

[11] Karp, F.B., Bernotski, N.A., Valdes, T.I., Böhringer, K.F., Ratner, Buddy, D. (2008). Foreign body response investigated with an implanted biosensor by in situ electrical impedance spectroscopy. *Sensors Journal, IEEE*, 8(1), 104–112.

[12] Nahvi, M. Hoyle, B.S. (2009). Electrical impedance spectroscopy sensing for industrial processes. *IEEE Sensors J.*, 9(12), 1808–1816.

[13] Widrow, B., Kollar, I. (2008). *Quantization noise*. Cambridge University Press.

[14] Ensheng, D., *et al.* (2010). A pulsed approach for electrical impedance spectroscopy measurement. *ISDEA* 2010, 1(150), 154, 13–14.

[15] Hoja, J., Lentka, G. (2013). A family of new generation miniaturized impedance analyzers for technical object diagnostics. *Metrol. Meas. Syst.*, 20(1), 43–52.

[16] Chabowski, K., Piasecki, T., Dzierka, A., Nitsch, K. (2015). Simple wide frequency range impedance meter based on AD5933 integrated circuit. *Metrol. Meas. Syst.*, 22(1), 13–24.

[17] Morrison, J.L., Morrison, W.H., Christophersen, J.P., Motloch, C.G. (2014). *Method of estimating pulse response using an impedance spectrum*. United States Patent.